



1 **Microbial dormancy and its impacts on Arctic terrestrial ecosystem carbon budget**

2

3 Junrong Zha and Qianlai Zhuang

4

5 Department of Earth, Atmospheric, and Planetary Sciences and Department of Agronomy,

6 Purdue University, West Lafayette, IN 47907 USA

7

8 Submitted to: *Biogeoscience*

9

10 Correspondence to: qzhuang@purdue.edu

11

12

13

14

15

16

17

18

19

20

21

22

23

24

25

26

27

28

29

30

31

32

33

34

35

36

37

38

39

40

41

42

43

44

45

46



47 **Abstract**

48 **A large amount of soil carbon in the Arctic terrestrial ecosystems could be emitted as**
49 **greenhouse gases in a warming future. However, lacking detailed microbial processes such**
50 **as microbial dormancy in current biogeochemistry models might have biased the**
51 **quantification of the regional carbon dynamics. Here the effect of microbial dormancy was**
52 **incorporated into a biogeochemistry model to improve the quantification for the last and**
53 **this century. Compared with the previous model without considering the microbial**
54 **dormancy, the new model estimated the regional soils stored 75.9 Pg more C in the**
55 **terrestrial ecosystems during the last century, and will store 50.4 Pg and 125.2 Pg more C**
56 **under the RCP 8.5 and RCP 2.6 scenarios, respectively, in this century. This study**
57 **highlights the importance of the representation of microbial dormancy in earth system**
58 **models to adequately quantify the carbon dynamics in the Arctic.**

59

60

61

62

63

64

65

66

67

68

69

70

71

72

73

74

75



76 1. Introduction

77 The land ecosystems in northern high latitudes ($>45^{\circ}$ N) occupy 22% of the global
78 surface and store over 40% of the global soil organic carbon (SOC) (McGuire & Hobbie, 1997;
79 Melillo et al., 1993; Tarnocai et al., 2009; Hugelius et al., 2014). During the past decades, a
80 greening accompanying a warming in the region has been documented (Zhou et al., 2001; Lloyd
81 et al., 2002; Stow et al., 2004; Callaghan et al., 2005; Tape et al., 2006). The regional carbon
82 dynamics are expected to loom large in the global carbon cycle and exert large feedbacks to the
83 global climate system (McGuire et al., 2009; Davidson & Janssens, 2006; Bond-Lamberty &
84 Thomson, 2010).

85 To date, numerous ecosystem models have been developed to project the feedbacks
86 between terrestrial ecosystem carbon cycling and climate (Raich et al., 1991; Zhuang et al.,
87 2001, 2002, 2015; Parton et al., 1993; Knorr et al., 2005; Running & Coughlan, 1988), but they
88 can bias their quantifications due to missing detailed microbial mechanisms in these models
89 (Schmidt et al., 2011; Todd-Brown et al., 2013; Conant et al., 2011; Treseder et al., 2011).
90 Microorganisms play a central role in decomposition of litter and soil organic carbon, which
91 further governs the global carbon cycling and climate change (Xu et al., 2014; Treseder et al.,
92 2011; Wang et al., 2015). An emerging field of research has begun to incorporate microbial
93 ecology into existing process-based models to remedy the inadequate representation of soil
94 decomposition process (Zha & Zhuang, 2018; Schimel & Weintraub, 2003; Allison et al., 2010;
95 German et al., 2012). These microbial-based models tend to better reproduce field and satellite
96 observations than traditional ones that treat soil decomposition as a first-order decay process
97 without considering microbial activities (Treseder et al., 2011; Wieder et al., 2013; Todd-Brown
98 et al., 2011; Lawrence et al., 2009; Moorhead et al., 2006). However, some vital microbial traits



99 such as microbial dormancy and community shifts are still rarely explicitly considered in large-
100 scale ecosystem models, and this may introduce notable uncertainties (Graham et al., 2014,
101 2016; Wang et al., 2015; Bouskill et al., 2012; Kaiser et al., 2014).

102 Dormancy is broadly recognized as a strategy for microorganisms to cope with periodical
103 environmental stresses (Harder & Dijkhuizen, 1983). When environmental conditions are
104 unfavorable for growth, microbes switch to a dormant state, which is a reversible state of low to
105 zero metabolic activity (Stolpovsky et al., 2011; Lennon & Jones, 2011). In this state,
106 biogeochemical processes such as soil decomposition are slow (Blagodatskaya et al., 2013). At
107 any given time, there is only a fraction of number of microbes, likely below 50% of live
108 microbes, in natural soils (Wang et al., 2015; Stolpovsky et al., 2011). Soil decomposition and
109 nutrient cycling mainly depend on these active microbes because only active ones can consume
110 organic matter and replicate themselves (Wang et al., 2015; Blagodatskaya et al., 2014). To date,
111 most existing biogeochemistry models used total microbial biomass as indicator of microbial
112 activities, rather than the active portion of microbial biomass, which could bias the estimates of
113 soil decomposition and ecosystem carbon budget (Hagerty et al., 2014; He et al., 2015).
114 Especially, the Arctic terrestrial ecosystems are nitrogen-limited, neglecting microbial dormancy
115 will lead to incorrect estimates of nitrogen availability through soil decomposition, failing to
116 capture nitrogen feedbacks to carbon dynamics (Wang et al., 2015; Stolpovsky et al., 2011;
117 Thullner et al., 2005). Thus, incorporating dormancy effects will improve model realism and
118 provide a better projection of the Arctic carbon dynamics.

119 This study incorporated the effects of microbial dormancy trait into an extant process-
120 based biogeochemistry model (MIC-TEM) (Zha & Zhuang, 2018; He et al., 2015). The dormant
121 and active microbial physiology has been considered explicitly in the new version of model



122 (MIC-TEM-dormancy). The revised model was parameterized, validated, and then applied to
123 evaluate the carbon dynamics during the last and this centuries in the Arctic terrestrial
124 ecosystems (north 45 °N above).

125

126 **2. Methods**

127 **2.1 Overview**

128 First, we describe how we developed the new model (MIC-TEM-dormancy) by
129 incorporating the microbial dormancy trait into an existing microbial-based biogeochemistry
130 model (MIC-TEM). Second, parameterization and validation of MIC-TEM-dormancy using
131 observed net ecosystem exchange data, and heterotrophic respiration data at representative sites
132 have been shown. Third, we applied the model to northern high latitudes (above 45 °N) for the 20th
133 and 21st centuries, to demonstrate the dormancy effects.

134

135 **2.2 Model description.**

136 A non-dormancy version of biogeochemistry model (MIC-TEM) has been developed by
137 incorporating a microbial module (Allison et al., 2010) into an extant large-scale biogeochemical
138 model (TEM) to explicitly (Zhuang et al., 2001, 2002, 2003) consider the effects of microbial
139 dynamics and enzyme kinetics on carbon dynamics (Zha & Zhuang, 2018). Here we further
140 advanced the MIC-TEM by incorporating algorithms that describe the effects of microbial
141 dormancy dynamics based on He et al. (2015). Different from He et al. (2015), in which
142 microbial module was driven with existing data of carbon stocks and fluxes, our study
143 incorporated the microbial module into an extant MIC-TEM that simulates carbon data
144 dynamically. This coupling enables us to extrapolate our model to whole northern high-latitudes



145 region, rather than only for temperate forest region in He et al. (2015). In our new model (MIC-
 146 TEM-dormancy), microbial biomass pool was divided into two fractions, including the dormant
 147 and active microbial biomass pools. The two microbial biomass pools and the reversible
 148 transition between them have been considered explicitly in the new model, which was ignored in
 149 MIC-TEM (Figure 1).

150 In previous MIC-TEM, heterotrophic respiration (R_H) is calculated as:

$$151 \quad R_H = \text{ASSIM} * (1 - \text{CUE}) \quad (1)$$

152 Where ASSIM and CUE represent microbial assimilation and carbon use efficiency, respectively.

153 For detailed carbon dynamics in MIC-TEM, see Zha & Zhuang (2018).

154 Here we revised MIC-TEM by incorporating microbial dormancy dynamics according to
 155 He et al. (2015). In the new model (MIC-TEM-dormancy), the soil heterotrophic respiration R_H is
 156 comprised of three parts: the maintenance respiration from the active and dormant microorganisms
 157 and the CO_2 production through the process of microbial assimilation (He et al., 2015):

$$158 \quad R_H = m_R Q_{10}^{\frac{\text{temp}-15}{10}} B_a + \beta m_R Q_{10}^{\frac{\text{temp}-15}{10}} B_d + \text{CO}_2 \quad (2)$$

159 where the first two terms are maintenance respiration from the active and dormant
 160 microorganisms, respectively. The last term is the CO_2 produced during the process of microbial
 161 assimilation.

162 For first two terms, B_a and B_d represents the active and dormant microbial biomass pool,
 163 respectively. The parameter m_R denotes the specific maintenance rate at active state (h^{-1}), and β
 164 is the ratio of dormant maintenance rate to active maintenance rate. Thus, βm_R denotes the
 165 maximum specific maintenance rate at dormant state. Temperature sensitivity was expressed as

166 the Q_{10} function ($Q_{10}^{\frac{\text{temp}-15}{10}}$), where temp is soil temperature at top 20 cm (units: °C).



167 For the third term, the CO₂ produced through microbial assimilation is calculated as in He et al.
 168 (2015) and Allison et al. (2010):

$$169 \quad \text{CO}_2 = \text{ASSIM} * (1 - Y_g) \quad (3)$$

170 Where ASSIM represents the variable of microbial assimilation and the parameter Y_g represents
 171 carbon use efficiency. Microbial assimilation (ASSIM) is calculated as in He et al. (2015):

$$172 \quad \text{ASSIM} = \frac{1}{Y_g} \frac{\Phi}{\alpha} m_R Q_{10enz}^{\frac{\text{temp}-15}{10}} B_a \left(\frac{\text{CN}_{\text{soil}}}{\text{CN}_{\text{mic}}} \right)^{0.6} \quad (4)$$

173 Here parameter α is called the maintenance weight (h⁻¹), CN_{soil} and CN_{mic} denotes the C:N ratio
 174 of soil and that of microbial biomass to consider substrate quality. Besides, Φ is called substrate
 175 saturation level and defined as in He et al. (2015) and Wang et al. (2014):

$$176 \quad \Phi = \frac{S}{K_s + S} \quad (5)$$

177 Where K_s is the half saturation constant for substrate uptake as indicated by the Michaelis–Menten
 178 kinetic, and S is soluble C substrates that are directly accessible for microbial assimilation (Wang
 179 et al., 2014). Here we quantified concentration of soluble C substrates that are directly accessible
 180 for microbial assimilation by using conceptual framework from Davidson et al. (2012):

$$181 \quad S = \text{Soluble C} * D_{\text{liq}} * \theta^3 \quad (6)$$

182 The term ‘Soluble C’ denotes the state variable of soluble carbon pool. D_{liq} is the diffusion
 183 coefficient of the substrate in the liquid phase, and is formulated as D_{liq} = 1/(1-BD/PD)³. BD is the
 184 bulk density and PD is the soil particle density. θ is the volumetric soil moisture.

185 Different from MIC-TEM, the transitions between active and dormant microbial biomass are
 186 included in MIC-TEM-dormancy. We used B_{a→d} and B_{d→a} denotes the transition from the active
 187 to dormant microbe and from the dormant to active microbe, respectively (He et al., 2015; Wang
 188 et al., 2014):



$$189 \quad B_{a \rightarrow d} = (1 - \Phi) m_R Q_{10mic}^{\frac{temp-15}{10}} B_a \quad (7)$$

$$190 \quad B_{d \rightarrow a} = \Phi m_R Q_{10mic}^{\frac{temp-15}{10}} B_d \quad (8)$$

191 Dormancy rate is affected by substrate availability (B_a , B_d), soil temperature (temp) and soil
 192 moisture (θ in Φ).

193 The active microbial biomass (B_a) is modeled as (He et al., 2015; Wang et al., 2014):

$$194 \quad \frac{dB_a}{dt} = ASSIM * Y_g - m_R Q_{10mic}^{\frac{temp-15}{10}} B_a - B_{a \rightarrow d} + B_{d \rightarrow a} - DEATH - EPROD \quad (9)$$

195 Where DEATH and EPROD denotes microbial biomass death and enzyme production, which are
 196 modeled as proportional to active microbial biomass with constant rates r_{death} and $r_{EnzProd}$ (Allison
 197 et al., 2010):

$$198 \quad DEATH = r_{death} * B_a \quad (10)$$

$$199 \quad EPROD = r_{EnzProd} * B_a \quad (11)$$

200 Where r_{death} and $r_{EnzProd}$ are the rate constants of microbial death and enzyme production,
 201 respectively.

202 The dormant microbial biomass (B_d) is modeled as (He et al., 2015; Wang et al., 2014):

$$203 \quad \frac{dB_d}{dt} = -\beta m_R Q_{10mic}^{\frac{temp-15}{10}} B_d + B_{a \rightarrow d} - B_{d \rightarrow a} \quad (12)$$

204 The Soluble C pool is modeled as (He et al., 2015; Allison et al., 2010):

$$205 \quad \frac{d \text{Soluble C}}{dt} = DECA Y - ASSIM + ELOSS + DEATH \quad (13)$$

206 Where DECA Y represents the enzymatic decay of soil organic carbon (SOC), and ELOSS
 207 represents the loss of enzyme.

208 DECA Y is regulated by enzyme biomass (ENZ), soil organic carbon (SOC), soil temperature, and
 209 substrate quality (He et al., 2015):



$$210 \quad \text{DECAY} = V_{\max} * Q_{10enz}^{\frac{\text{temp}-15}{10}} * \text{ENZ} * \frac{\text{SOC}}{K_{m\text{uptake}} + \text{SOC}} * (120 - \text{CN}_{\text{soil}}) \quad (14)$$

211 Where V_{\max} is the maximum SOC decay rate, $K_{m\text{uptake}}$ is half saturation constant for enzymatic
 212 decay.

213 ELOSS is modeled as a first-order process (Allison et al., 2010) to represent enzyme turnover:

$$214 \quad \text{ELOSS} = r_{\text{enzloss}} * \text{ENZ} \quad (15)$$

215 Where r_{enzloss} is the rate constant of enzyme loss.

216 The soil organic carbon pool (SOC) is modeled as:

$$217 \quad \frac{d\text{SOC}}{dt} = \text{Litterfall} - \text{DECAY} \quad (16)$$

218 Where Litterfall is estimated as a function of vegetation carbon (Zhuang et al., 2010).

219 Last, enzyme pool (ENZ) is modeled as:

$$220 \quad \frac{d\text{ENZ}}{dt} = \text{EPROD} - \text{ELOSS} \quad (17)$$

221 With the modification of microbial carbon dynamics by considering microbial life-history trait,
 222 soil decomposition is changed since it is controlled by microbes. When microbial dormancy is
 223 considered, the number of active microbes that participate in soil decomposition is different. The
 224 changes in soil decomposition directly influence the amount of soil respiration, and further
 225 influence soil nitrogen (N) mineralization that determines soil N availability for plants, affecting
 226 gross primary production (GPP). Since both GPP and soil respiration (R_H) can be affected by
 227 microbial dormancy, net ecosystem production (NEP) will also be affected.

228

229 **2.3 Model parameterization and validation**

230 The detailed description of parameters that are related to microbial dormancy can be found
 231 in He et al. (2015) (Table 1). Here we calibrated the MIC-TEM-dormancy at six representative



232 sites with gap-filled monthly net ecosystem productivity (NEP, $\text{gCm}^{-2}\text{mon}^{-1}$) data in northern high
233 latitudes (Table 2). Site-level climatic data and soil texture data were organized for driving model.
234 All sites information can be found on AmeriFlux network (Davidson et al., 2000). The results for
235 model parameterization were presented in Figure 2. We conducted the parameterization using a
236 global optimization algorithm known as SCE-UA (Shuffled complex evolution) method (Duan et
237 al., 1994). An ensemble of 50 independent sets of parameters were performed based on prior ranges
238 from literature (Table 1) to minimize the difference between the monthly simulated and measured
239 NEP at the chosen sites. The cost function of the minimization is:

$$240 \quad \text{Obj} = \sum_{i=1}^k (\text{NEP}_{\text{obs},i} - \text{NEP}_{\text{sim},i})^2 \quad (17)$$

241 Where $\text{NEP}_{\text{obs},i}$ and $\text{NEP}_{\text{sim},i}$ are the observed and simulated NEP, respectively. k is the number of
242 data pairs for comparison. Except for the parameters of microbial dormancy, other parameters are
243 derived directly from MIC-TEM (Zha & Zhuang, 2018). The optimized parameters were used for
244 model validation and regional simulations.

245 For model validation, we chose another six sites that containing monthly NEP data from
246 AmeriFlux network (Table 3). Moreover, we also conducted site-level validations with monthly
247 soil respiration data from AmeriFlux network and Fluxnet dataset. The site information was
248 provided in Table 4. For these sites, we assumed 50% of soil respiration was heterotrophic
249 respiration (R_H) for forest (Hanson et al., 2000), 60% and 70% of that was R_H for grassland (Wang
250 et al., 2009) and tundra (Billings et al., 1977). Because there is a limited amount of measured data
251 of heterotrophic respiration, we could not conduct a regional validation for all pixels in northern
252 high latitudes. Instead, we extracted 61 sites providing data of average annual heterotrophic
253 respiration from ORNL global Soil Respiration Dataset
254 (https://daac.ornl.gov/SOILS/guides/SRDB_V4.html, Bond-Lamberty et al., 2018) for model



255 validation. The site-level observed average annual R_H was used to compare with simulated annual
256 R_H by MIC-TEM-dormancy and MIC-TEM. The new model (MIC-TEM-dormancy) was run at
257 monthly time step to keep consistent with the time step of MIC-TEM. Although microbial
258 dynamics occur at fine temporal scales (Tang & Riley, 2014), we can still quantify the cumulative
259 impacts of microbial dynamics on carbon and nitrogen cycling at monthly time by not changing
260 the model structure.

261

262 **2.4 Spatial extrapolation**

263 For historical simulations during the 20th century, two sets of regional simulations using
264 MIC-TEM-dormancy and MIC-TEM at a spatial resolution of 0.5° latitude \times 0.5° longitude were
265 conducted. Our model simulation contains two parts: spin-up and transient simulation. A typical
266 spin-up was conducted to get the model to a steady state for each spatial location, which will be
267 used as initial conditions for transient simulations (McGuire et al., 1992). During spin-up
268 procedure, cyclic forcing data was used to force the model run, and repeated continuously until
269 dynamic equilibrium was achieved at which the modeled state variables show a cyclic pattern or
270 become constant. Specifically, this study used the monthly historical climate data from 1900 to
271 1940 to repeatedly drive the model for the spin-up. Before spin-up procedure, the model was
272 initialized with default built-in carbon stocks (Raich et al., 1991). During transient simulations,
273 the calibrated ecosystem-specific parameters were used for regional simulations. The previous
274 dynamic equilibrium was used as initial value for transient simulation. The historical climatic
275 forcing data, including the monthly air temperature, precipitation, cloudiness, and atmospheric
276 CO_2 concentrations, were organized from the Climatic Research Unit (CRU TS3.1) from the
277 University of East Anglia (Harris et al., 2014). Gridded data of soil texture (Zhuang et al., 2003),



278 elevation (Zhuang et al., 2015), and potential natural vegetation (Melillo et al., 1993) from
279 literatures were also used. In our model, we assumed that soil texture, elevation, and potential
280 natural vegetation data only vary spatially, not vary over time (Zhuang et al., 2015).

281 In addition, regional simulations over the 21st century were conducted under two
282 Intergovernmental Panel on Climate Change (IPCC) climate scenarios (RCP 2.6 and RCP 8.5).
283 The future climatic forcing data under these two climate change scenarios were derived from the
284 HadGEM2-ESmodel, which is a member of CMIP5project213 ([https://esgf-
285 node.llnl.gov/search/cmip5/](https://esgf-node.llnl.gov/search/cmip5/)). Then the regional estimations were obtained by summing up the
286 gridded outputs for our study region. The positive simulated NEP represents a CO₂ sink from the
287 atmosphere to terrestrial ecosystems, while a negative value represents a source of CO₂ from
288 terrestrial ecosystems to the atmosphere.

289

290 **3. Results**

291 **3.1 Inversed Model Parameters and model validation**

292 Using SCE-UA ensemble method, 50 independent sets of parameters were converged to
293 minimize the objective function. Then the optimized parameters are calculated as the mean of these
294 50 sets of inversed parameters. The boxplot of parameter posterior distributions reflects different
295 ecosystem properties at these sites (Figure 3). For instance, carbon use efficiency (CUE) was much
296 higher in tundra types than in forests, meaning microorganisms in environment with higher energy
297 limitation tend to enhance the efficiency of energy transportation. Besides, alpha, the maintenance
298 weight, was also much higher in tundra types than in forests. The opposite can be seen from
299 parameter beta, the ratio of dormant maintenance rate to specific maintenance rate for active



300 biomass. Other microbial related parameters did not differentiate much among different vegetation
301 types.

302 After parameterization, the MIC-TEM-dormancy was validated with monthly NEP data for
303 six representative ecosystems, and the comparisons between monthly observed NEP and
304 simulated NEP were presented in Figure 4. With the optimized parameters, the dormancy-based
305 model was used to reproduce NEP to compare with the measured NEP (Table 5). The statistical
306 analysis shows that R^2 ranges from 0.67 for Atqasuk to 0.93 for Bartlett Experimental Forest
307 (Table 5). Generally, our new model performs better for forest ecosystems than for tundra
308 ecosystems. Compared with MIC-TEM, which is no dormancy-based, dormancy model performs
309 better for alpine tundra, temperate coniferous forest, and grassland. For other sites, two models
310 show similar performance (Table 5). Another set of sites with monthly soil respiration data were
311 selected to conduct model validation. The comparisons between monthly observed R_H and
312 simulated R_H from two contrasting models were conducted (Figure 5). MIC-TEM-dormancy has
313 higher R^2 and lower RMSE (Table 6). Sixty-one sites with average annual R_H in northern high-
314 latitude region were used to further evaluate the new model performance. The dormancy model
315 has lower intercept and slope with R^2 of 0.45, while R^2 of MIC-TEM is 0.3 (Figure 6). These
316 analyses indicate that new model is more realistic in representing heterotrophic respiration (R_H)
317 by considering microbial dormancy. This difference further affects soil available nitrogen
318 dynamics, influencing nitrogen uptake by plants, the rate of photosynthesis and NPP.

319

320 **3.2 Regional carbon dynamics during the 20th century**

321 Regional extrapolation with both models estimated a regional carbon sink but with different
322 magnitudes (Figure 7c). Here positive values of NEP represent sinks of CO_2 into terrestrial



323 ecosystems, while negative values represent sources of CO₂ to the atmosphere. With optimized
324 parameters, MIC-TEM estimated a regional carbon sink of 77.6 Pg with the interannual standard
325 deviation of 0.21 Pg C yr⁻¹ during the 20th century. However, MIC-TEM-dormancy nearly doubles
326 the sink at 153.5 Pg with the interannual standard deviation of 0.12 Pg C yr⁻¹ during the last
327 century, which estimates 75.9 Pg more carbon sink than MIC-TEM does but with less interannual
328 variation (Figure 7c). At the end of the century, MIC-TEM estimated that NEP reaches 1.0 Pg C
329 yr⁻¹ in comparison with MIC-TEM-dormancy estimates of 1.5 Pg C yr⁻¹ (Figure 7c). Both models
330 simulated similar trends for regional NPP, R_H and NEP (Figure 7). Generally, they show an
331 increasing trend in the 20th century except a slight decrease during the 1960s (Figure 7).
332 Meanwhile, with optimized parameters, MIC-TEM-dormancy estimated NPP and R_H at 7.94 Pg C
333 yr⁻¹ and 6.4 Pg C yr⁻¹, which are 5.8% and 16.3% less than the estimations from MIC-TEM,
334 respectively (Figures 7a and 7b). This pronounced difference of NEP between two models comes
335 from the disparity between the simulated NPP and R_H with them. Without considering dormancy,
336 MIC-TEM estimates more active microbial biomass since it assumes the whole microbial biomass
337 pool will participate in soil decomposition. The fact is only active part of microbial biomass can
338 work for soil decomposition, meaning MIC-TEM overestimates R_H. On the other hand,
339 Overestimation of R_H can induce higher nitrogen uptake by plants, which will accelerate rate of
340 photosynthesis and further enhance NPP projection. Although MIC-TEM estimates higher NPP
341 and R_H than MIC-TEM-dormancy does, NEP estimated from MIC-TEM is actually lower.

342 The average annual seasonal patterns of NPP, R_H and NEP during the 1990s were also
343 organized from regional simulations with two models (Figure 8). Temporally, both two models
344 projected higher NPP and R_H in summer than in winter (Figures 8a and 8b) due to higher soil
345 temperature and moisture (McGuire et al., 1992). MIC-TEM produced less R_H in winter but



346 higher R_H in summer than MIC-TEM-dormancy (Figure 8b), which indicates that without
347 dormancy, model tends to estimate lower soil respiration compared to dormancy model due to
348 ignorance of dormant respiration in winter but estimate higher soil respiration due to higher
349 estimation of active biomass in summer. In the meantime, seasonal cycle of NPP with MIC-
350 TEM-dormancy shows a relative flattening pattern compared with MIC-TEM, which is similar to
351 seasonal cycle of R_H (Figure 8a). This is because higher R_H can cause higher NPP due to the
352 reasons we have mentioned above. Though R_H and NPP show the similar seasonal patterns, NEP
353 can still show different pattern since it's the difference between NPP and R_H . Here seasonal
354 cycles of NEP with models are close to each other (Figure 8c), but dormancy model projected
355 slightly higher NEP in summer. Besides, setting the R_H projection from MIC-TEM as baseline,
356 MIC-TEM-dormancy averagely projected 33% less R_H in summer (May to September), and 30%
357 more in winter (other months). This suggested that relative difference of R_H between two models
358 in summer was higher than in winter.

359 **3.3 Regional carbon dynamics during the 21st century**

360 Under the RCP 8.5 scenario, both models estimated the region acts as a carbon sink
361 (Figure 9). The MIC-TEM-dormancy predicted that the sink is 129.9 Pg with the interannual
362 standard deviation of 0.13 Pg C yr⁻¹, whereas MIC-TEM estimates the sink is 79.5 Pg with the
363 interannual standard deviation of 0.37 Pg C yr⁻¹ during the 21st century (Figure 9). Thus, MIC-
364 TEM-dormancy estimates an increase of 50.4 Pg regional carbon sequestration relative to MIC-
365 TEM but with less interannual variation (Figure 9). Both models predict similar temporal trends
366 for NEP, namely increasing from the 2000s and then decreasing from the 2070s onward (Figure
367 9). MIC-TEM-dormancy predicts that carbon sink reaches 1.36 Pg C yr⁻¹ in the 2090s, which is
368 0.26 Pg C yr⁻¹ more than projection of MIC-TEM. Moreover, MIC-TEM-dormancy estimated



369 NPP and R_H at $10.2 \text{ Pg C yr}^{-1}$ and 8.9 Pg C yr^{-1} , which are 1.3 Pg C yr^{-1} and 1.8 Pg C yr^{-1} less
370 than the estimations from MIC-TEM, respectively (Figure 9). Under the RCP 2.6 scenario, the
371 cumulative NEP from two models diverged by 125.2 Pg C by 2100. The trajectory of inter-
372 annual NEP estimated with the two models also diverged. The MIC-TEM predicted the region
373 fluctuates between carbon sinks and sources, and totally acts as a carbon source of 1.6 Pg C with
374 the interannual standard deviation of $0.24 \text{ Pg C yr}^{-1}$ during the 21st century. In contrast, MIC-
375 TEM-dormancy projected the region acts as a carbon sink of 123.6 Pg C with the interannual
376 standard deviation of 0.1 Pg C yr^{-1} (Figure 9). MIC-TEM-dormancy estimates NPP and R_H at 9.9
377 Pg C yr^{-1} and 8.7 Pg C yr^{-1} , which are 0.5 Pg C yr^{-1} and 1.7 Pg C yr^{-1} less than the estimations
378 from MIC-TEM, respectively (Figure 9).

379 The average annual seasonal patterns of NPP, R_H and NEP during the 2990s by two models were
380 also presented (Figure 10). MIC-TEM-dormancy estimated higher R_H in winter, but lower R_H in
381 summer under both future scenarios (Figure 10). Similar seasonal cycle pattern appears for NPP
382 projection. The combined flattening patterns of NPP and R_H result in different patterns for NEP.
383 Under the RCP 2.6 scenario, MIC-TEM-dormancy predicts higher NEP from June to October,
384 but similar NEP in other months to MIC-TEM (Figure 10). Under the RCP 8.5 scenario, MIC-
385 TEM-dormancy predicts higher NEP from June to September, but much lower NEP in other
386 months than MIC-TEM (Figure 10).

387 **4. Discussion**

388 Soils are the largest carbon repository in the terrestrial biosphere and hold 2.5 times more
389 carbon than the atmosphere (Frey et al., 2013; Schlesinger & Andrews, 2000). Especially, a
390 significant portion of soil organic carbon currently stored in northern high latitudes region
391 (Tarnocai et al., 2009). Besides, climate over this region has warmed in recent decades (Serreze



392 & Francis, 2006) and the changing climate is expected to alter the carbon cycle through
393 influencing the activities of microorganisms in controlling soil decomposition (Manzoni et al.,
394 2012; Melillo et al., 2011). Therefore, explicit consideration of microbial traits and functions in
395 large-scale biogeochemistry models is necessary for better quantification of carbon-climate
396 feedbacks (Thullner et al., 2005; Wang et al., 2015). Our regional simulations with two
397 contrasting models (MIC-TEM, MIC-TEM-dormancy) indicate the region was a carbon sink in
398 past decades, which is consistent with results from other process-based models (White et al.,
399 2000; Houghton et al., 2007; McGuire et al., 2009; Schimel, 2013). However, the magnitudes of
400 this sink are quite different in two models. Moreover, MIC-TEM-dormancy predicts the sink will
401 decrease under both RCP 8.5 and RCP 2.6 scenarios during the 21st century, while MIC-TEM
402 projects that the sink will increase under the RCP 8.5 but change to carbon source under the RCP
403 2.6 scenario. The large difference in two models suggests the importance of incorporating
404 microbial dormancy effects.

405 The large bias between dormancy and non-dormancy models mainly comes from two parts.
406 First, most important microbial activities such as soil organic carbon decomposition and nutrient
407 cycling largely depend on the active fraction of microbial communities, not total microbial
408 biomass (Wang et al., 2014; Blagodatsky et al., 2000). However, only a small part (about 0.1-
409 2%, seldom exceed 5%) of the total soil microbial biomass is recognized to be active under
410 natural conditions (Blagodatsky et al., 2011; Werf & Verstraete, 1987). Thus, dormancy could be
411 a prominent feature in soil systems (Wang et al., 2014). Without considering dormancy, the
412 “effective” microbial biomass for soil decomposition could be overestimated, resulting in
413 overestimation of heterotrophic respiration (He et al., 2015). Our regional estimate of R_H is 6.4
414 Pg C yr^{-1} during the 20th century by MIC-TEM-dormancy, while 7.7 Pg C yr^{-1} by MIC-TEM. No



415 dormancy model simulated 20.3% higher respiration than dormancy model. For future
416 simulations, MIC-TEM-dormancy predicted 8.7 Pg C yr⁻¹ and 9.0 Pg C yr⁻¹ of R_H under RCP 2.6
417 and RCP 8.5 scenarios during the 21st century, respectively. Nevertheless, no dormancy model
418 simulated 19.5% and 21.2% higher respiration than dormancy model under RCP 2.6 and RCP 8.5
419 scenarios, respectively. He et al. (2015) predicted total soil R_H of all temperate forests (25°N-
420 50°N) from the dormancy model amounted to 7.28 Pg C yr⁻¹ and 8.83 Pg C yr⁻¹ from a no-
421 dormancy model, which is 21.3% higher than the dormancy model. Although their study region
422 and simulation period are different from our study, the results can still be comparable. Both
423 studies indicated that the magnitude of R_H and proportion from no-dormancy model are higher
424 than dormancy models. Second, high soil respiration stimulates N mineralization in soils
425 (Zhuang et al., 2001, 2002), making more nutrients for photosynthesis of plants (Raich et al.,
426 1991; McGuire et al., 1995). Therefore, NPP will be higher due to the N enrichment from higher
427 R_H. However, how NEP will change is still unclear. Our regional estimate of NEP during the 20th
428 century by MIC-TEM-dormancy is 1.54 Pg C yr⁻¹, and is 0.78 Pg C yr⁻¹ by MIC-TEM. Schimel
429 et al. (2001) reported that a range of estimates of the northern extratropical NEP is from 0.6 to
430 2.3 PgC yr⁻¹ in the 1980s. In comparison with our estimates of 1.61 Pg C yr⁻¹ with MIC-TEM-
431 dormancy and 0.84 Pg C yr⁻¹ with MIC-TEM, our regional estimates of NEP are in reasonable
432 range. Moreover, our predicted trend of NEP is very similar to the finding of White et al. (2000),
433 indicating that NEP increases from the 2000s to the 2070s, and then decreases in the 2090s.
434 Moreover, future simulations under two contrasting climate scenarios (RCP 2.6 and RCP 8.5)
435 exhibit a large difference of 81.1 Pg C of cumulative NEP during the 21st century by MIC-TEM,
436 but only 6.3 Pg C of that by MIC-TEM-dormancy. This difference indicates microbes provide a
437 resistant response to climate change due to dormancy to some extent (Treseder et al., 2011).



438 Although our dormancy model can project reasonable carbon fluxes and indicate the
439 importance of incorporating microbial dormancy when compared with no dormancy model
440 (MIC-TEM; Zha & Zhuang et al., 2018), there are some other microbial traits have not yet been
441 considered in our model. For instance, one vital common evolutionary trait of microbe is the
442 community shift (Wang et al., 2015) with changing environment, including warming, N
443 fertilization and precipitation (Treseder et al., 2011; Frey et al., 2013; Allison et al., 2009; Evans
444 & Wallenstein, 2011). Community shift will influence microbial physiology, temperature
445 sensitivity and growth rates (Classen et al., 2015), which will further affect the rate of soil
446 decomposition and other carbon dynamics (Treseder et al., 2011; Schimel & Schaeffer, 2012;
447 Todd-Brown et al., 2011). Moreover, microbial acclimation is another important trait to affect
448 soil decomposition. Recent studies have found the capacity of the microbial community to
449 maintain the warming-induced elevated respiration could decrease over time because of
450 acclimation (Melillo et al. 1993; Todd-Brown et al., 2011). This mechanism of adaption to a new
451 temperature regime shall be factored into future soil decomposition analysis. Besides, microbial
452 community composition was ignored in our model. We didn't separate among functional
453 microbial groups, but gather microbes into one "box". However, microbial community
454 composition could influence ecosystem functioning, and their variance in responses to
455 environmental conditions could alter the prediction of the rates of decomposition of organic
456 material (Balsler et al. 2002; Fierer et al. 2007). Especially, some narrowly-distributed functions
457 can be more sensitive to microbial community composition, and these might benefit most from
458 explicit consideration of distinguishing functional groups in ecosystem models (McGuire &
459 Treseder, 2010; Schimel 1995). Thus, functional dissimilarity in microbial communities can be
460 considered in next step for model development (Strickland et al., 2009; Moorhead et al., 2006).



461 Except for above model limitations, additional uncertainties may come from inadequate
462 model parameterization and model assumptions. For example, a critical microbial parameter,
463 carbon use efficiency (CUE), is a primary control to soil CO₂ efflux. Higher CUE indicates more
464 microbial growth and more carbon uptake by plants, while lower CUE indicates higher soil
465 decomposition (Manzoni et al., 2012). Theoretical and empirical studies have suggested that
466 CUE depends on both temperature and substrate quality (Frey et al., 2013) and decreases as
467 temperature increases and nutrient availability decreases (Manzoni et al., 2012). Our study
468 considered the CUE sensitivity to temperature, but not nutrient availability. On the other hand,
469 some model assumptions can also cause uncertainties. For example, we assumed that vegetation
470 will not change during the transient simulation. However, over the past few decades in northern
471 high latitudes, temperature increases have led to vegetation shift from one type to another
472 (Hansen et al., 2006; White et al., 2000). The vegetation changes will affect carbon cycling in
473 these ecosystems.

474

475 5. Conclusions

476 This study incorporated microbial dormancy into a detailed microbial-based soil
477 decomposition biogeochemistry model to examine the fate of large Arctic soil carbon under
478 changing climate conditions. Regional simulations using MIC-TEM-dormancy indicated that,
479 over the 20th century, the region is a carbon sink of 153.5 Pg. This sink could decrease to 129.9
480 Pg under the RCP 8.5 scenario or 123.6 Pg under the RCP 2.6 scenario during the 21st century.
481 Whether considering microbial dormancy or not can cause large differences in soil
482 decomposition estimation between two models. Meanwhile, due to available nitrogen affected by
483 soil decomposition, net primary production is consequently influenced in these two centuries.



484 The combined changes in soil decomposition and net primary production led to large differences
485 in carbon budget estimation between two models. Compared with MIC-TEM, MIC-TEM-
486 dormancy projected 75.9 Pg more C stored in the terrestrial ecosystems over the last century,
487 50.4 Pg and 125.2 Pg more C under the RCP 8.5 and RCP 2.6 scenarios, respectively. This study
488 highlights the importance of the representation of microbial dormancy in earth system models in
489 order to adequately quantify the carbon dynamics in northern high latitudes.

490

491 **Acknowledgments**

492 This research was supported by a NSF project (IIS-1027955), a DOE project (DE-SC0008092),
493 and a NASA LCLUC project (NNX09AI26G) to Q. Z. We acknowledge the Rosen High
494 Performance Computing Center at Purdue for computing support. We thank the National Snow
495 and Ice Data center for providing Global Monthly EASE-Grid Snow Water Equivalent data,
496 National Oceanic and Atmospheric Administration for North American Regional Reanalysis
497 (NARR). We also acknowledge the World Climate Research Programme's Working Group on
498 Coupled Modeling Intercomparison Project CMIP5, and we thank the climate modeling groups
499 for producing and making available their model output. The data presented in this paper can be
500 accessed through our research website (<http://www.eaps.purdue.edu/ebdl/>)

501

502

503 **References:**

504 Allison, E. H., Perry, A. L., Badjeck, M.-C., Neil Adger, W., Brown, K., Conway, D., Halls, A.
505 S., Pilling, G. M., Reynolds, J. D., Andrew, N. L., and Dulvy, N. K.: Vulnerability of national
506 economies to the impacts of climate change on fisheries, *Fish and Fisheries*, 10, 173-196,
507 10.1111/j.1467-2979.2008.00310.x, 2009.
508 Allison, S. D., Wallenstein, M. D., and Bradford, M. A.: Soil-carbon response to warming
509 dependent on microbial physiology, *Nature Geoscience*, 3, 336-340, 10.1038/ngeo846, 2010.
510 Balser, T. C., Kinzig, A. P., and Firestone, M. K.: Linking soil microbial communities and
511 ecosystem functioning, *The functional consequences of biodiversity: Empirical progress and
512 theoretical extensions*, 265-293, 2002.



- 513 Blagodatskaya, E., and Kuzyakov, Y.: Active microorganisms in soil: Critical review of
514 estimation criteria and approaches, *Soil Biology and Biochemistry*, 67, 192-211,
515 10.1016/j.soilbio.2013.08.024, 2013.
- 516 Blagodatskaya, E., Khomyakov, N., Myachina, O., Bogomolova, I., Blagodatsky, S., and
517 Kuzyakov, Y.: Microbial interactions affect sources of priming induced by cellulose, *Soil
518 Biology and Biochemistry*, 74, 39-49, 10.1016/j.soilbio.2014.02.017, 2014.
- 519 Blagodatsky, S., Grote, R., Kiese, R., Werner, C., and Butterbach-Bahl, K.: Modelling of
520 microbial carbon and nitrogen turnover in soil with special emphasis on N-trace gases emission,
521 *Plant and soil*, 346, 297-330, 10.1007/s11104-011-0821-z, 2011.
- 522 Blagodatsky, S. A., Heinemeyer, O., and Richter, J.: Estimating the active and total soil
523 microbial biomass by kinetic respiration analysis, *Biol Fertil Soils*, 32, 73-81, 2000.
- 524 Bond-Lamberty, B., and Thomson, A.: Temperature-associated increases in the global soil
525 respiration record, *Nature*, 464, 579-582, 10.1038/nature08930, 2010.
- 526 Bond-Lamberty, B., Bailey, V. L., Chen, M., Gough, C. M., and Vargas, R.: Globally rising soil
527 heterotrophic respiration over recent decades, *Nature*, 560, 80-83, 10.1038/s41586-018-0358-x,
528 2018.
- 529 Bouskill, N. J., Tang, J., Riley, W. J., and Brodie, E. L.: Trait-based representation of biological
530 nitrification: model development, testing, and predicted community composition, *Frontiers in
531 microbiology*, 3, 364, 10.3389/fmicb.2012.00364, 2012.
- 532 Callaghan, T., Björn, L. O., Chernov, Y., Chapin, T., Christensen, T. R., Huntley, B., Ims, R.,
533 Jolly, D., Jonasson, S., Matveyeva, N., Panikov, N., Oechel, W., and Shaver, G.: Arctic tundra
534 and polar desert ecosystems, *Arctic climate impact assessment*, 243-352, 2005.
- 535 Carney, K. M., and Matson, P. A.: The influence of tropical plant diversity and composition on
536 soil microbial communities, *Microbial ecology*, 52, 226-238, 10.1007/s00248-006-9115-z, 2006.
- 537 Chmlelewrki, R. A. N., and Frank, J. F.: Formation of viable but nonculturable *Salmonella*
538 during starvation in chemically defined solutions, *Letters in Applied Microbiology*, 20, 380-384,
539 1995.
- 540 Classen, A. T., Sundqvist, M. K., Henning, J. A., Newman, G. S., Moore, J. A. M., Cregger, M.
541 A., Moorhead, L. C., and Patterson, C. M.: Direct and indirect effects of climate change on soil
542 microbial and soil microbial-plant interactions: What lies ahead?, *Ecosphere*, 6, art130,
543 10.1890/es15-00217.1, 2015.
- 544 Conant, R. T., Ryan, M. G., Ågren, G. I., Birge, H. E., Davidson, E. A., Eliasson, P. E., Evans, S.
545 E., Frey, S. D., Giardina, C. P., Hopkins, F. M., Hyvönen, R., Kirschbaum, M. U. F., Lavelle, J.
546 M., Leifeld, J., Parton, W. J., Megan Steinweg, J., Wallenstein, M. D., Martin Wetterstedt, J. Å.,
547 and Bradford, M. A.: Temperature and soil organic matter decomposition rates - synthesis of
548 current knowledge and a way forward, *Global change biology*, 17, 3392-3404, 10.1111/j.1365-
549 2486.2011.02496.x, 2011.
- 550 Coursolle, C., Margolis, H. A., Barr, A. G., Black, T. A., Amiro, B. D., McCaughey, J. H.,
551 Flanagan, L. B., Lafleur, P. M., Roulet, N. T., Bourque, C. P. A., Arain, M. A., Wofsy, S. C.,
552 Dunn, A., Morgenstern, K., Orchansky, A. L., Bernier, P. Y., Chen, J. M., Kidston, J., Saigusa,
553 N., and Hedstrom, N.: Late-summer carbon fluxes from Canadian forests and peatlands along an
554 east-west continental transect, *Canadian Journal of Forest Research*, 36, 783-800, 10.1139/x05-
555 270, 2006.
- 556 Davidson, E. A., Trumbore, S. E., and Amundson, R.: Biogeochemistry: soil warming and
557 organic carbon content, *Nature*, 408, 2000.



- 558 Davidson, E. A., and Janssens, I. A.: Temperature sensitivity of soil carbon decomposition and
559 feedbacks to climate change, *Nature*, 440, 165-173, 10.1038/nature04514, 2006.
- 560 Davidson, E. A., Janssens, I. A., and Luo, Y.: On the variability of respiration in terrestrial
561 ecosystems: moving beyond Q₁₀, *Global change biology*, 12, 154-164, 10.1111/j.1365-
562 2486.2005.01065.x, 2006.
- 563 Davidson, E. A., Samanta, S., Caramori, S. S., and Savage, K.: The Dual Arrhenius and
564 Michaelis-Menten kinetics model for decomposition of soil organic matter at hourly to seasonal
565 time scales, *Global change biology*, 18, 371-384, 10.1111/j.1365-2486.2011.02546.x, 2012.
- 566 Duan, Q., Sorooshian, S., and Gupta, V. K.: Optimal use of the SCE-UA global optimization
567 method for calibrating watershed models, *Journal of Hydrology*, 158, 265-284, 1994.
- 568 Evans, S. E., and Wallenstein, M. D.: Soil microbial community response to drying and
569 rewetting stress: does historical precipitation regime matter?, *Biogeochemistry*, 109, 101-116,
570 10.1007/s10533-011-9638-3, 2011.
- 571 Fierer, N., Morse, J. L., Berthrong, S. T., Bernhardt, E. S., and Jackson, R. B.: Environmental
572 controls on the landscape - scale biogeography of stream bacterial communities, *Ecology*, 88,
573 2162-2173, 2007.
- 574 Frey, S. D., Lee, J., Melillo, J. M., and Six, J.: The temperature response of soil microbial
575 efficiency and its feedback to climate, *Nature Climate Change*, 3, 395-398,
576 10.1038/nclimate1796, 2013.
- 577 Gangsheng Wang, M. A. M., Lianhong Gu, Christopher W. Schadt: Representation of Dormant
578 and Active Microbial Dynamics for Ecosystem Modeling, *Public Library of Science*, 9,
579 10.1371/journal.pone.0089252.g001, 2014.
- 580 German, D. P., Marcelo, K. R. B., Stone, M. M., and Allison, S. D.: The Michaelis-Menten
581 kinetics of soil extracellular enzymes in response to temperature: a cross-latitudinal study,
582 *Global change biology*, 18, 1468-1479, 10.1111/j.1365-2486.2011.02615.x, 2012.
- 583 Gilmanov, T. G., Tieszen, L. L., Wylie, B. K., Flanagan, L. B., Frank, A. B., Haferkamp, M. R.,
584 Meyers, T. P., and Morgan, J. A.: Integration of CO₂ flux and remotely-sensed data for primary
585 production and ecosystem respiration analyses in the Northern Great Plains: potential for
586 quantitative spatial extrapolation, *Global Ecology and Biogeography*, 14, 271-292,
587 10.1111/j.1466-822X.2005.00151.x, 2005.
- 588 Gough, C. M., Hardiman, B. S., Nave, L. E., Bohrer, G., Maurer, K. D., Vogel, C. S.,
589 Nadelhoffer, K. J., and Curtis, P. S.: Sustained carbon uptake and storage following moderate
590 disturbance in a Great Lakes forest, *Ecological Applications*, 23, 1202-1215, 2013.
- 591 Goulden, M. L., Winston, G. C., McMillan, A. M. S., Litvak, M. E., Read, E. L., Rocha, A. V.,
592 and Rob Elliot, J.: An eddy covariance mesonet to measure the effect of forest age on
593 land-atmosphere exchange, *Global change biology*, 12, 2146-2162, 10.1111/j.1365-
594 2486.2006.01251.x, 2006.
- 595 Graham, E. B., Wieder, W. R., Leff, J. W., Weintraub, S. R., Townsend, A. R., Cleveland, C. C.,
596 Philippot, L., and Nemergut, D. R.: Do we need to understand microbial communities to predict
597 ecosystem function? A comparison of statistical models of nitrogen cycling processes, *Soil
598 Biology and Biochemistry*, 68, 279-282, 10.1016/j.soilbio.2013.08.023, 2014.
- 599 Graham, E. B., Knelman, J. E., Schindlbacher, A., Siciliano, S., Breulmann, M., Yannarell, A.,
600 Beman, J. M., Abell, G., Philippot, L., Prosser, J., Foulquier, A., Yuste, J. C., Glanville, H. C.,
601 Jones, D. L., Angel, R., Salminen, J., Newton, R. J., Burgmann, H., Ingram, L. J., Hamer, U.,
602 Siljanen, H. M., Peltoniemi, K., Potthast, K., Banerjee, L., Hartmann, M., Banerjee, S., Yu, R. Q.,
603 Nogaro, G., Richter, A., Koranda, M., Castle, S. C., Goberna, M., Song, B., Chatterjee, A.,



- 604 Nunes, O. C., Lopes, A. R., Cao, Y., Kaisermann, A., Hallin, S., Strickland, M. S., Garcia-
605 Pausas, J., Barba, J., Kang, H., Isobe, K., Papaspyrou, S., Pastorelli, R., Lagomarsino, A.,
606 Lindstrom, E. S., Basiliko, N., and Nemergut, D. R.: Microbes as Engines of Ecosystem
607 Function: When Does Community Structure Enhance Predictions of Ecosystem Processes?,
608 *Frontiers in microbiology*, 7, 214, 10.3389/fmicb.2016.00214, 2016.
- 609 Griffis, T. J., Lee, X., Baker, J. M., Billmark, K., Schultz, N., Erickson, M., Zhang, X.,
610 Fassbinder, J., Xiao, W., and Hu, N.: Oxygen isotope composition of evapotranspiration and its
611 relation to C₄photosynthetic discrimination, *Journal of Geophysical Research*, 116,
612 10.1029/2010jg001514, 2011.
- 613 Hagerty, S. B., van Groenigen, K. J., Allison, S. D., Hungate, B. A., Schwartz, E., Koch, G. W.,
614 Kolka, R. K., and Dijkstra, P.: Accelerated microbial turnover but constant growth efficiency
615 with warming in soil, *Nature Climate Change*, 4, 903-906, 10.1038/nclimate2361, 2014.
- 616 Hansen, J., Sato, M., Ruedy, R., Lo, K., Lea, D. W., and Medina-Elizade, M.: Global
617 temperature change, *Proceedings of the National Academy of Sciences of the United States of*
618 *America*, 103, 14288-14293, 10.1073/pnas.0606291103, 2006.
- 619 Harder, w., and Dijkhuizen, L.: Physiological responses to nutrient limitation, *Annual Review of*
620 *Microbiology*, 37, 1983.
- 621 Harris, I., Jones, P. D., Osborn, T. J., and Lister, D. H.: Updated high-resolution grids of monthly
622 climatic observations - the CRU TS3.10 Dataset, *International Journal of Climatology*, 34, 623-
623 642, 10.1002/joc.3711, 2014.
- 624 He, Y., Yang, J., Zhuang, Q., Harden, J. W., McGuire, A. D., Liu, Y., Wang, G., and Gu, L.:
625 Incorporating microbial dormancy dynamics into soil decomposition models to improve
626 quantification of soil carbon dynamics of northern temperate forests, *Journal of Geophysical*
627 *Research: Biogeosciences*, 120, 2596-2611, 10.1002/2015jg003130, 2015.
- 628 Hiller, R. V., McFadden, J. P., and Kljun, N.: Interpreting CO₂ Fluxes Over a Suburban Lawn:
629 The Influence of Traffic Emissions, *Boundary-Layer Meteorology*, 138, 215-230,
630 10.1007/s10546-010-9558-0, 2010.
- 631 Houghton, R. A.: Balancing the Global Carbon Budget, *Annual Review of Earth and Planetary*
632 *Sciences*, 35, 313-347, 10.1146/annurev.earth.35.031306.140057, 2007.
- 633 Hugelius, G., Strauss, J., Zubrzycki, S., Harden, J. W., Schuur, E. A. G., Ping, C. L.,
634 Schirrmeister, L., Grosse, G., Michaelson, G. J., Koven, C. D., amp, apos, Donnell, J. A.,
635 Elberling, B., Mishra, U., Camill, P., Yu, Z., Palmtag, J., and Kuhry, P.: Estimated stocks of
636 circumpolar permafrost carbon with quantified uncertainty ranges and identified data gaps,
637 *Biogeosciences*, 11, 6573-6593, 10.5194/bg-11-6573-2014, 2014.
- 638 Jenkins, J. P., Richardson, A. D., Braswell, B. H., Ollinger, S. V., Hollinger, D. Y., and Smith,
639 M. L.: Refining light-use efficiency calculations for a deciduous forest canopy using
640 simultaneous tower-based carbon flux and radiometric measurements, *Agricultural and Forest*
641 *Meteorology*, 143, 64-79, 10.1016/j.agrformet.2006.11.008, 2007.
- 642 Kaiser, C., Franklin, O., Dieckmann, U., and Richter, A.: Microbial community dynamics
643 alleviate stoichiometric constraints during litter decay, *Ecology letters*, 17, 680-690,
644 10.1111/ele.12269, 2014.
- 645 Knorr, W., Prentice, I. C., House, J. I., and Holland, E. A.: Long-term sensitivity of soil carbon
646 turnover to warming, *Nature*, 433, 2005.
- 647 Lawrence, C. R., Neff, J. C., and Schimel, J. P.: Does adding microbial mechanisms of
648 decomposition improve soil organic matter models? A comparison of four models using data



- 649 from a pulsed rewetting experiment, *Soil Biology and Biochemistry*, 41, 1923-1934,
650 [10.1016/j.soilbio.2009.06.016](https://doi.org/10.1016/j.soilbio.2009.06.016), 2009.
- 651 Lennon, J. T., and Jones, S. E.: Microbial seed banks: the ecological and evolutionary
652 implications of dormancy, *Nature reviews. Microbiology*, 9, 119-130, [10.1038/nrmicro2504](https://doi.org/10.1038/nrmicro2504),
653 2011.
- 654 Lloyd, A. H., Rupp, T. S., Fastie, C. L., and Starfield, A. M.: Patterns and dynamics of treeline
655 advance on the Seward Peninsula, Alaska, *Journal of Geophysical Research*, 108,
656 [10.1029/2001jd000852](https://doi.org/10.1029/2001jd000852), 2002.
- 657 Manzoni, S., Taylor, P., Richter, A., Porporato, A., and Agren, G. I.: Environmental and
658 stoichiometric controls on microbial carbon-use efficiency in soils, *The New phytologist*, 196,
659 79-91, [10.1111/j.1469-8137.2012.04225.x](https://doi.org/10.1111/j.1469-8137.2012.04225.x), 2012.
- 660 McEwing, K. R., Fisher, J. P., and Zona, D.: Environmental and vegetation controls on the
661 spatial variability of CH₄ emission from wet-sedge and tussock tundra ecosystems in the Arctic,
662 *Plant and soil*, 388, 37-52, [10.1007/s11104-014-2377-1](https://doi.org/10.1007/s11104-014-2377-1), 2015.
- 663 McGuire, A. D., Melillo, J. M., Joyce, L. A., Kicklighter, D. W., Grace, A. L., III, B. M., and
664 Vorosmarty, C. J.: Interactions between carbon and nitrogen dynamics in estimating net primary
665 productivity for potential vegetation in North America, *Global Biogeochemical Cycles*, 6, 101-
666 124, 1992.
- 667 McGuire, A. D., Melillo, J. M., Kicklighter, D. W., and Joyce, L. A.: Equilibrium responses of
668 soil carbon to climate change: Empirical and process-based estimates, *Journal of Biogeography*,
669 22, 785-796, 1995.
- 670 McGuire, A. D., and Hobbie, J. E.: Global climate change and the equilibrium responses of
671 carbon storage in arctic and subarctic regions, In *Modeling the Arctic system: A workshop report*
672 *on the state of modeling in the Arctic System Science program*, 53-54, 1997.
- 673 McGuire, A. D., Anderson, L. G., Christensen, T. R., Dallimore, S., Guo, L., Hayes, D. J.,
674 Heimann, M., Lorensen, T. D., Macdonald, R. W., and Roulet, N.: Sensitivity of the carbon
675 cycle in the Arctic to climate change, *Ecological Monographs*, 79, 523-555, 2009.
- 676 McGuire, K. L., and Treseder, K. K.: Microbial communities and their relevance for ecosystem
677 models: Decomposition as a case study, *Soil Biology and Biochemistry*, 42, 529-535,
678 [10.1016/j.soilbio.2009.11.016](https://doi.org/10.1016/j.soilbio.2009.11.016), 2010.
- 679 Me'tris, A., Gerrard, A. M., Cumming, R. H., Weigner, P., and Paca, J.: Modelling shock
680 loadings and starvation in the biofiltration of toluene and xylene, *Journal of Chemical*
681 *Technology and Biotechnology*, 76, 565-572, 2001.
- 682 Melillo, J. M., McGuire, A. D., Kicklighter, D. W., III, B. M., Vorosmarty, C. J., and Schloss, A.
683 L.: Global climate change and terrestrial net primary production, *Nature*, 363, 1993.
- 684 Melillo, J. M., Butler, S., Johnson, J., Mohan, J., Steudler, P., Lux, H., Burrows, E., Bowles, F.,
685 Smith, R., Scott, L., Vario, C., Hill, T., Burton, A., Zhou, Y.-M., and Tang, J.: Soil warming,
686 carbon - nitrogen interactions, and forest carbon budgets, *PNAS*, 108, 9508-9512, 2011.
- 687 Merbold, L., Kutsch, W. L., Corradi, C., Kolle, O., Rebmann, C., Stoy, P. C., Zimov, S. A., and
688 Schulze, E. D.: Artificial drainage and associated carbon fluxes (CO₂/CH₄) in a tundra
689 ecosystem, *Global change biology*, 15, 2599-2614, [10.1111/j.1365-2486.2009.01962.x](https://doi.org/10.1111/j.1365-2486.2009.01962.x), 2009.
- 690 Moorhead, D. L., and Sinsabaugh, R. L.: A theoretical model of litter decay and microbial
691 interaction, *Ecological Monographs*, 76, 151-174, 2006.
- 692 Oechel, W. C., Laskowski, C. A., Burba, G., Gioli, B., and Kalhori, A. A. M.: Annual patterns
693 and budget of CO₂ flux in an Arctic tussock tundra ecosystem, *Journal of Geophysical Research:*
694 *Biogeosciences*, 119, 323-339, [10.1002/2013jg002431](https://doi.org/10.1002/2013jg002431), 2014.



- 695 P.J. Hanson, N. T. E., C.T. Garten, J.A. Andrews: Separating root and soil microbial
696 contributions to soil respiration: A review of methods and observations, *Biogeochemistry*, 48,
697 115-146, 2000.
- 698 Parton, W. J., Scurlock, J. M. O., Ojima, D. S., Gilmanov, T. G., Scholes, R. J., Schimel, D. S.,
699 Kirchner, T., Menaut, J. C., Seastedt, T., Moya, E. G., Kamnalrut, A., and Kinyamario, J. I.:
700 Observations and modeling of biomass and soil organic matter dynamics for the grassland biome
701 worldwide, *Global Biogeochemical Cycles*, 7, 785-809, 1993.
- 702 Raich, J. W., Rastetter, E. B., Melillo, J. M., Kicklighter, D. W., Steudler, P. A., Peterson, B. J.,
703 Grace, A. L., III, B. M., and Vorosmarty, C. J.: Potential net primary productivity in South
704 America: application of a global model, *Ecological Applications*, 1, 399-429, 1991.
- 705 Richardson, A. D., Jenkins, J. P., Braswell, B. H., Hollinger, D. Y., Ollinger, S. V., and Smith,
706 M. L.: Use of digital webcam images to track spring green-up in a deciduous broadleaf forest,
707 *Oecologia*, 152, 323-334, [10.1007/s00442-006-0657-z](https://doi.org/10.1007/s00442-006-0657-z), 2007.
- 708 Running, S. W., and Coughlan, J. C.: A general model of forest ecosystem processes for regional
709 applications I. Hydrologic balance, canopy gas exchange and primary production processes.,
710 *Ecological Modelling*, 42, 125-154, 1988.
- 711 Schimel, D. S.: Terrestrial ecosystems and the carbon cycle, *Global change biology*, 1, 77-91,
712 1995.
- 713 Schimel, D. S., House, J. I., Hibbard, K. A., Bousquet, P., Ciais, P., Peylin, P., Braswell, B. H.,
714 Apps, M. J., Baker, D., Bondeau, A., Canadell, J., Churkina, G., Cramer, W., Denning, A. S.,
715 Field, C. B., Friedlingstein, P., Goodale, C., Heimann, M., Houghton, R. A., Melillo, J. M., III,
716 B. M., Murdiyarso, D., Noble, I., Pacala, S. W., Prentice, I. C., Raupach, M. R., Rayner, P. J.,
717 Scholes, R. J., Steffen, W. L., and Wirth, C.: Recent patterns and mechanisms of carbon
718 exchange by terrestrial ecosystems, *Nature*, 414, 2001.
- 719 Schimel, J.: Microbes and global carbon, *Nature Climate Change*, 3, 867-868,
720 [10.1038/nclimate2015](https://doi.org/10.1038/nclimate2015), 2013.
- 721 Schimel, J. P., and Weintraub, M. N.: The implications of exoenzyme activity on microbial
722 carbon and nitrogen limitation in soil: a theoretical model, *Soil Biology and Biochemistry*, 35,
723 549-563, [10.1016/s0038-0717\(03\)00015-4](https://doi.org/10.1016/s0038-0717(03)00015-4), 2003.
- 724 Schimel, J. P., and Schaeffer, S. M.: Microbial control over carbon cycling in soil, *Frontiers in*
725 *microbiology*, 3, 348, [10.3389/fmicb.2012.00348](https://doi.org/10.3389/fmicb.2012.00348), 2012.
- 726 Schlesinger, W. H., and Andrews, J. A.: Soil respiration and the global carbon cycle,
727 *Biogeochemistry*, 48, 7-20, 2000.
- 728 Schmidt, M. W., Torn, M. S., Abiven, S., Dittmar, T., Guggenberger, G., Janssens, I. A., Kleber,
729 M., Kogel-Knabner, I., Lehmann, J., Manning, D. A., Nannipieri, P., Rasse, D. P., Weiner, S.,
730 and Trumbore, S. E.: Persistence of soil organic matter as an ecosystem property, *Nature*, 478,
731 49-56, [10.1038/nature10386](https://doi.org/10.1038/nature10386), 2011.
- 732 Serreze, M. C., and Francis, J. A.: The Arctic on the fast track of change, *Weather*, 61, 65-69,
733 2006.
- 734 Stolpovsky, K., Martinez-Lavanchy, P., Heipieper, H. J., Van Cappellen, P., and Thullner, M.:
735 Incorporating dormancy in dynamic microbial community models, *Ecological Modelling*, 222,
736 3092-3102, [10.1016/j.ecolmodel.2011.07.006](https://doi.org/10.1016/j.ecolmodel.2011.07.006), 2011.
- 737 Stow, D. A., Hope, A., McGuire, D., Verbyla, D., Gamon, J., Huemmrich, F., Houston, S.,
738 Racine, C., Sturm, M., Tape, K., Hinzman, L., Yoshikawa, K., Tweedie, C., Noyle, B.,
739 Silapaswan, C., Douglas, D., Griffith, B., Jia, G., Epstein, H., Walker, D., Daeschner, S.,
740 Petersen, A., Zhou, L., and Myneni, R.: Remote sensing of vegetation and land-cover change in



- 741 Arctic Tundra Ecosystems, *Remote Sensing of Environment*, 89, 281-308,
742 10.1016/j.rse.2003.10.018, 2004.
- 743 Strickland, M. S., Lauber, C., Fierer, N., and Bradford, M. A.: Testing the functional
744 significance of microbial community composition, *Ecology*, 90, 441-451, 2009.
- 745 Tang, J., and Riley, W. J.: Weaker soil carbon–climate feedbacks resulting from microbial and
746 abiotic interactions, *Nature Climate Change*, 5, 56-60, 10.1038/nclimate2438, 2014.
- 747 Tape, K. E. N., Sturm, M., and Racine, C.: The evidence for shrub expansion in Northern Alaska
748 and the Pan-Arctic, *Global change biology*, 12, 686-702, 10.1111/j.1365-2486.2006.01128.x,
749 2006.
- 750 Tarnocai, C., Canadell, J. G., Schuur, E. A. G., Kuhry, P., Mazhitova, G., and Zimov, S.: Soil
751 organic carbon pools in the northern circumpolar permafrost region, *Global Biogeochemical*
752 *Cycles*, 23, n/a-n/a, 10.1029/2008gb003327, 2009.
- 753 Thullner, M., Van Cappellen, P., and Regnier, P.: Modeling the impact of microbial activity on
754 redox dynamics in porous media, *Geochimica et Cosmochimica Acta*, 69, 5005-5019,
755 10.1016/j.gca.2005.04.026, 2005.
- 756 Todd-Brown, K. E. O., Hopkins, F. M., Kivlin, S. N., Talbot, J. M., and Allison, S. D.: A
757 framework for representing microbial decomposition in coupled climate models,
758 *Biogeochemistry*, 109, 19-33, 10.1007/s10533-011-9635-6, 2011.
- 759 Todd-Brown, K. E. O., Randerson, J. T., Post, W. M., Hoffman, F. M., Tarnocai, C., Schuur, E.
760 A. G., and Allison, S. D.: Causes of variation in soil carbon simulations from CMIP5 Earth
761 system models and comparison with observations, *Biogeosciences*, 10, 1717-1736, 10.5194/bg-
762 10-1717-2013, 2013.
- 763 Treseder, K. K., Balsler, T. C., Bradford, M. A., Brodie, E. L., Dubinsky, E. A., Eviner, V. T.,
764 Hofmockel, K. S., Lennon, J. T., Levine, U. Y., MacGregor, B. J., Pett-Ridge, J., and Waldrop,
765 M. P.: Integrating microbial ecology into ecosystem models: challenges and priorities,
766 *Biogeochemistry*, 109, 7-18, 10.1007/s10533-011-9636-5, 2011.
- 767 W. D. Billings, K. M. P., G. R. Shaver, A. W. Trent: Root Growth, Respiration, and Carbon
768 Dioxide Evolution in an Arctic Tundra Soil, *Arctic and Alpine Research*, 9, 129-137,
769 10.1080/00040851.1977.12003908, 1977.
- 770 Wang, G., Jagadamma, S., Mayes, M. A., Schadt, C. W., Steinweg, J. M., Gu, L., and Post, W.
771 M.: Microbial dormancy improves development and experimental validation of ecosystem
772 model, *The ISME journal*, 9, 226-237, 10.1038/ismej.2014.120, 2015.
- 773 Wang Wei, F. J., T. Oikawa: Contribution of Root and Microbial Respiration to Soil CO₂ Efflux
774 and Their Environmental Controls in a Humid Temperate Grassland of Japan, *Pedosphere*, 19,
775 31-39, 2009.
- 776 Werf, H. V. d., and Verstraete, W.: Estimation of active soil microbial biomass by mathematical
777 analysis of respiration curves: relation to conventional estimation of total biomass, *Soil Biology*
778 *and Biochemistry*, 19, 267-271, 1987.
- 779 White, A., Cannell, M. G. R., and Friend, A. D.: The high-latitude terrestrial carbon sink: a
780 model analysis *Global change biology*, 6, 227-245, 2000.
- 781 Wieder, W. R., Bonan, G. B., and Allison, S. D.: Global soil carbon projections are improved by
782 modelling microbial processes, *Nature Climate Change*, 3, 909-912, 10.1038/nclimate1951,
783 2013.
- 784 Xu, X., Schimel, J. P., Thornton, P. E., Song, X., Yuan, F., and Goswami, S.: Substrate and
785 environmental controls on microbial assimilation of soil organic carbon: a framework for Earth
786 system models, *Ecology letters*, 17, 547-555, 10.1111/ele.12254, 2014.



787 Zha, J., and Zhuang, Q.: Microbial decomposition processes and vulnerable arctic soil organic
788 carbon in the 21st century, *Biogeosciences*, 15, 5621-5634, 10.5194/bg-15-5621-2018, 2018a.
789 Zha, J., and Zhuang, Q.: Microbial decomposition processes and vulnerable Arctic soil organic
790 carbon in the 21st century, *Biogeosciences Discussions*, 1-34, 10.5194/bg-2018-241, 2018b.
791 Zhou, L., Tucker, C. J., Kaufmann, R. K., Slayback, D., Shabanov, N. V., and Myneni, R. B.:
792 Variations in northern vegetation activity inferred from satellite data of vegetation index during
793 1981 to 1999, *Journal of Geophysical Research: Atmospheres*, 106, 20069-20083,
794 10.1029/2000jd000115, 2001.
795 Zhuang, Q., Romanovsky, V. E., and McGuire, A. D.: Incorporation of a permafrost model into a
796 large-scale ecosystem model: Evaluation of temporal and spatial scaling issues in simulating soil
797 thermal dynamics, *Journal of Geophysical Research: Atmospheres*, 106, 33649-33670,
798 10.1029/2001jd900151, 2001.
799 Zhuang, Q., McGuire, A. D., O'Neill, K. P., Harden, J. W., Romanovsky, V. E., and Yarie, J.:
800 Modeling soil thermal and carbon dynamics of a fire chronosequence in interior Alaska, *Journal*
801 *of Geophysical Research*, 108, 10.1029/2001jd001244, 2002.
802 Zhuang, Q., He, J., Lu, Y., Ji, L., Xiao, J., and Luo, T.: Carbon dynamics of terrestrial
803 ecosystems on the Tibetan Plateau during the 20th century: an analysis with a process-based
804 biogeochemical model, *Global Ecology and Biogeography*, 19, 649-662, 10.1111/j.1466-
805 8238.2010.00559.x, 2010.
806 Zhuang, Q., Zhu, X., He, Y., Prigent, C., Melillo, J. M., David McGuire, A., Prinn, R. G., and
807 Kicklighter, D. W.: Influence of changes in wetland inundation extent on net fluxes of carbon
808 dioxide and methane in northern high latitudes from 1993 to 2004, *Environmental Research*
809 *Letters*, 10, 095009, 10.1088/1748-9326/10/9/095009, 2015.
810 Zhuang, Q., McGuire, A. D., Melillo, J. M., Clein, J. S., Dargaville, R. J., Kicklighter, D. W.,
811 Myneni, R. B., Dong, J., Romanovsky, V. E., Harden, J., and Hobbie, J. E.: Carbon cycling in
812 extratropical terrestrial ecosystems of the Northern Hemisphere during the 20th century: a
813 modeling analysis of the influences of soil thermal dynamics, *Tellus B: Chemical and Physical*
814 *Meteorology*, 55, 751-776, 10.3402/tellusb.v55i3.16368, 2016.
815
816
817
818

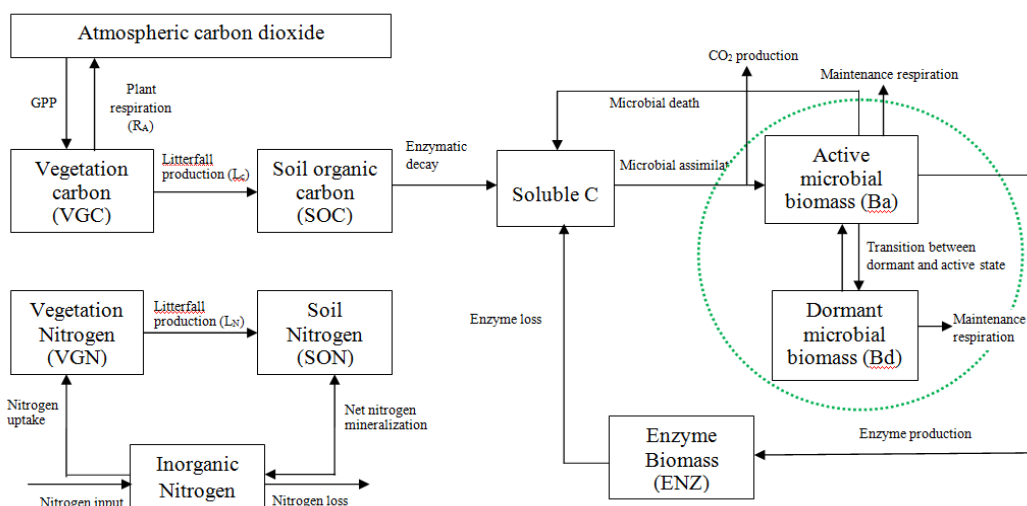
819 **Author contributions.** Q.Z. designed the study. J.Z. conducted model development, simulation
820 and analysis. J.Z. and Q. Z. wrote the paper.

821 **Competing financial interests.** The submission has no competing financial interests.

822 **Materials & Correspondence.** Correspondence and material requests should be addressed to
823 qzhuang@purdue.edu.

824

825



826

827

828

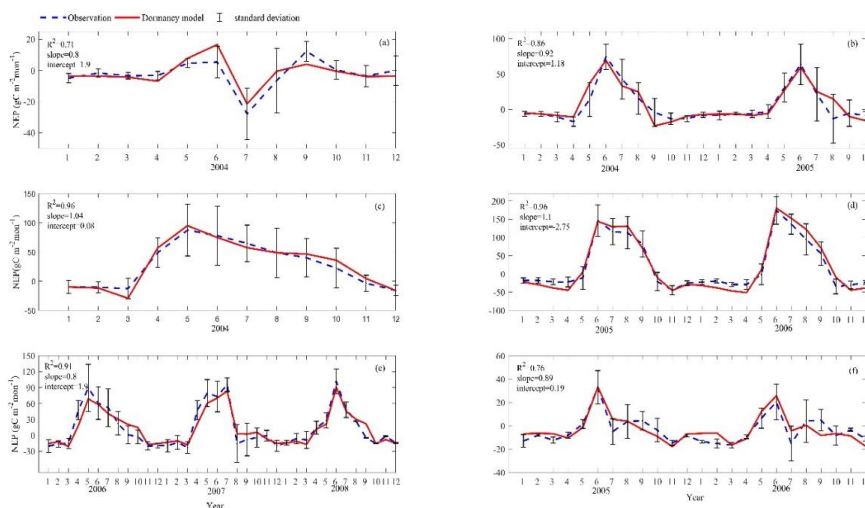
829

830

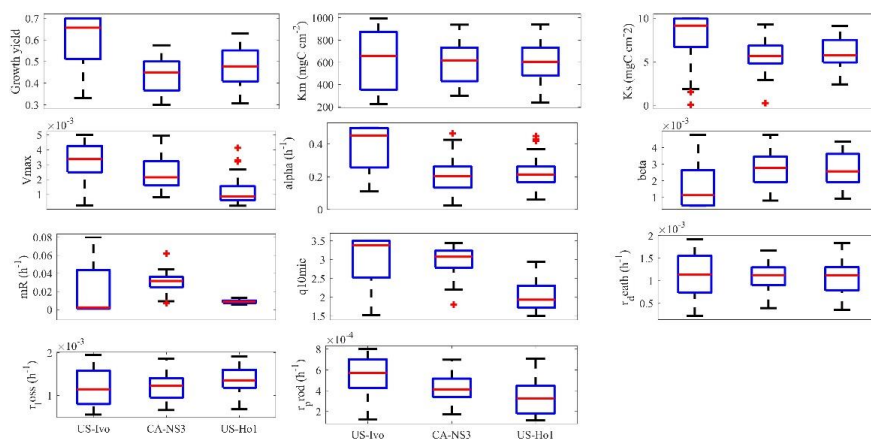
831

832

Figure 1. Framework of the dormancy model: microbial biomass is split into two parts, active microbial biomass and dormant microbial biomass (shown in the green dashed circle). Maintenance respiration from these two parts, and the CO₂ production through microbial assimilation contributes to heterotrophic respiration. The model was revised based on Zha & Zhuang (2018).



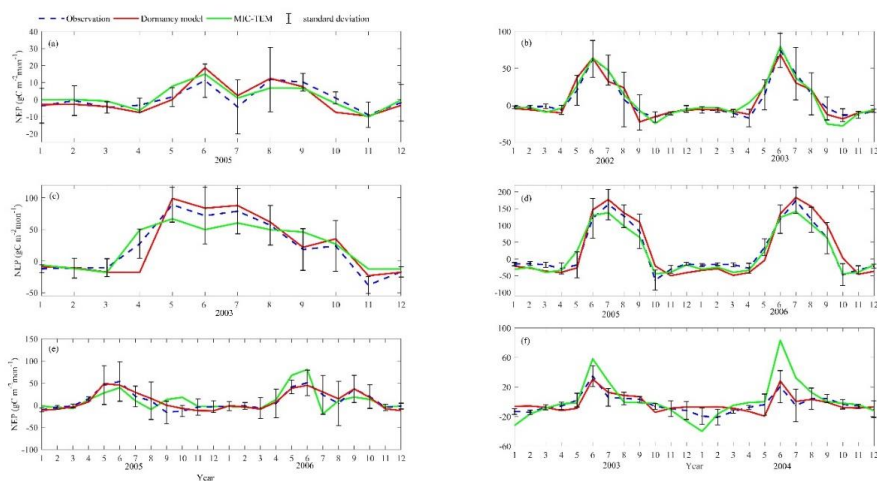
833
 834 Figure 2. Comparison between observed and simulated NEP ($\text{gC m}^{-2}\text{mon}^{-1}$) at: (a) Ivotuk (alpine
 835 tundra), (b) UCI-1964 burn site (boreal forest), (c) Howland Forest (main tower) (temperate
 836 coniferous forest), (d) Univ. of Mich. Biological Station (Temperate deciduous forest), (e)
 837 KUOM Turfgrass Field (Grassland), and (f) Atqasuk (Wet tundra). Note: scales are different.
 838 Error bars represent standard errors among daily measure data in one month.
 839



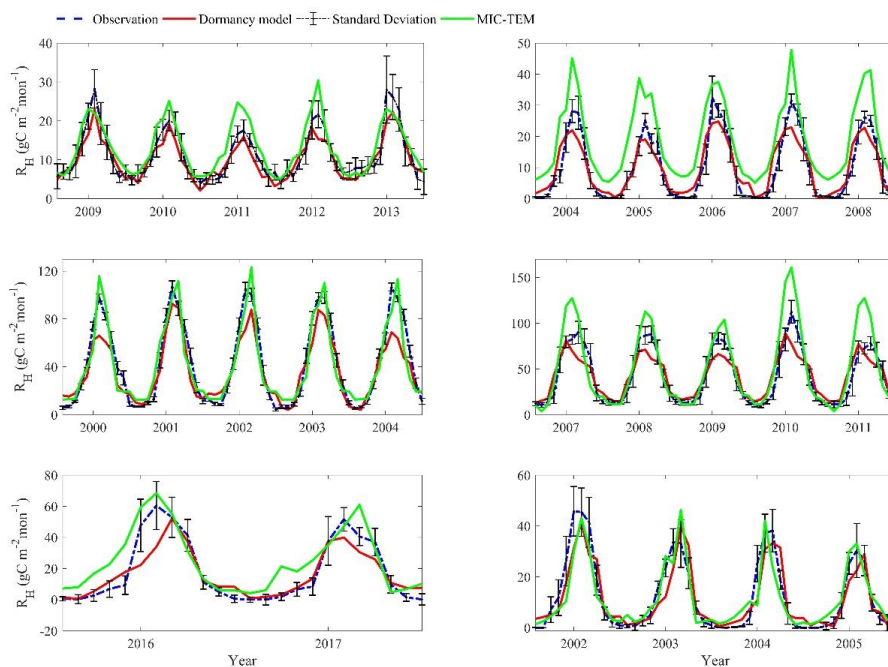
840

841 Figure 3. Boxplot of parameter posterior distribution that are obtained after ensemble inverse
 842 modeling for MIC-TEM-dormancy all six sites: US-Ivo: Ivotuk (alpine tundra), CA-NS3: UCI-
 843 1964 burn site (boreal forest), US-Ho1: Howland Forest (temperate coniferous forest), US-UMB:
 844 Univ. of Mich. Biological Station (temperate deciduous forest), US-KUT: KUOM Turfgrass
 845 Field (grassland), US-Atq: Atqasuk (wet tundra).

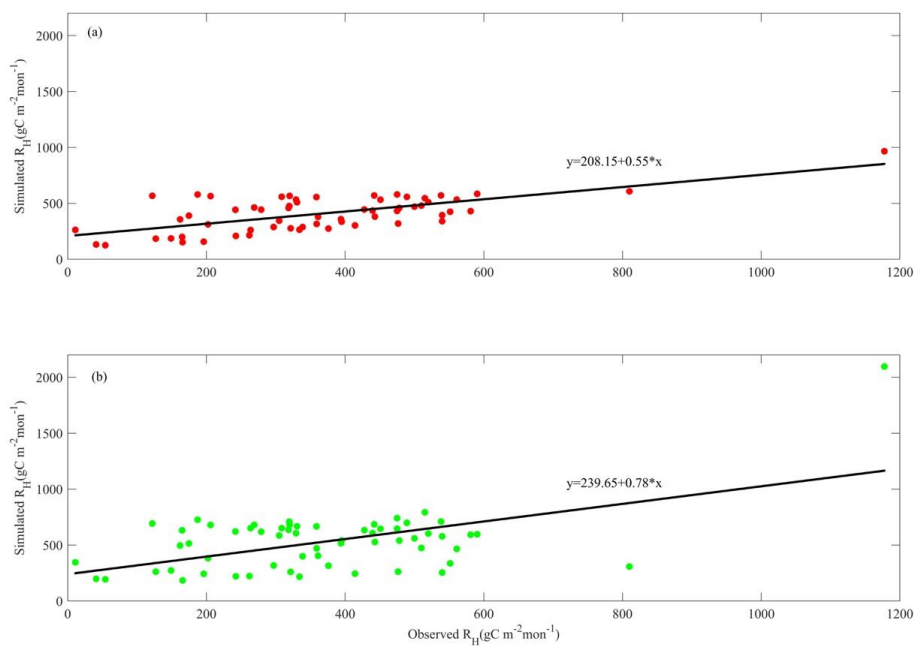
846



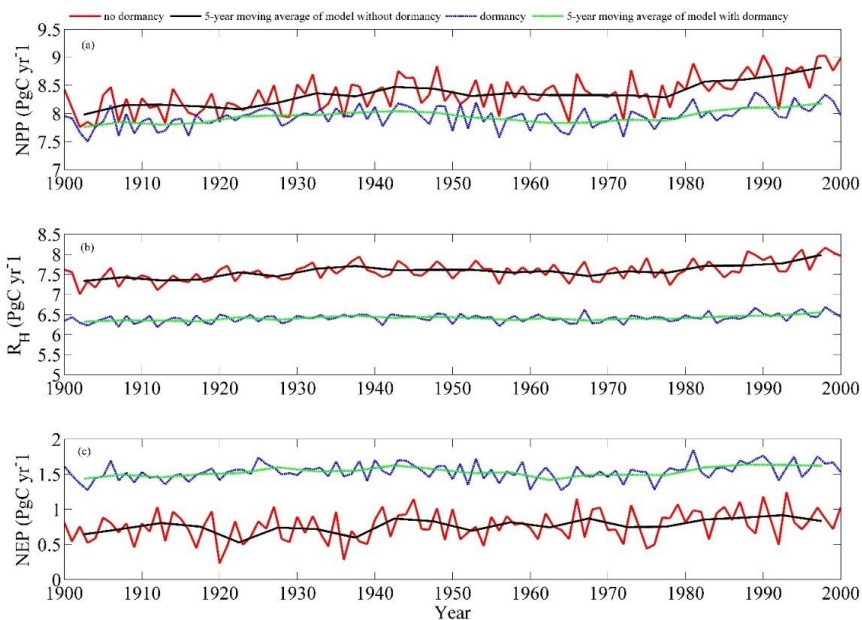
847
848 Figure 4. Comparison between observed and simulated NEP ($\text{gC m}^{-2}\text{mon}^{-1}$) at: (a) Iivotuk (alpine
849 tundra), (b) UCI-1964 burn site (boreal forest), (c) Howland Forest (main tower) (temperate
850 coniferous forest), (d) Bartlett Experimental Forest (Temperate deciduous forest), (e) Brookings
851 (Grassland), and (f) Atqasuk (Wet tundra). Note: scales are different.
852



853
854 Figure 5. Comparison between observed and simulated R_H ($\text{gC m}^{-2}\text{mon}^{-1}$) at: (a) US-EML (alpine
855 tundra), (b) CA-SJ2 (boreal forest), (c) US-Ho2 (temperate coniferous forest), (d) US-UMB
856 (Temperate deciduous forest), (e) US-Ro4 (Grassland), and (f) RU-Che (Wet tundra). Note:
857 scales are different.

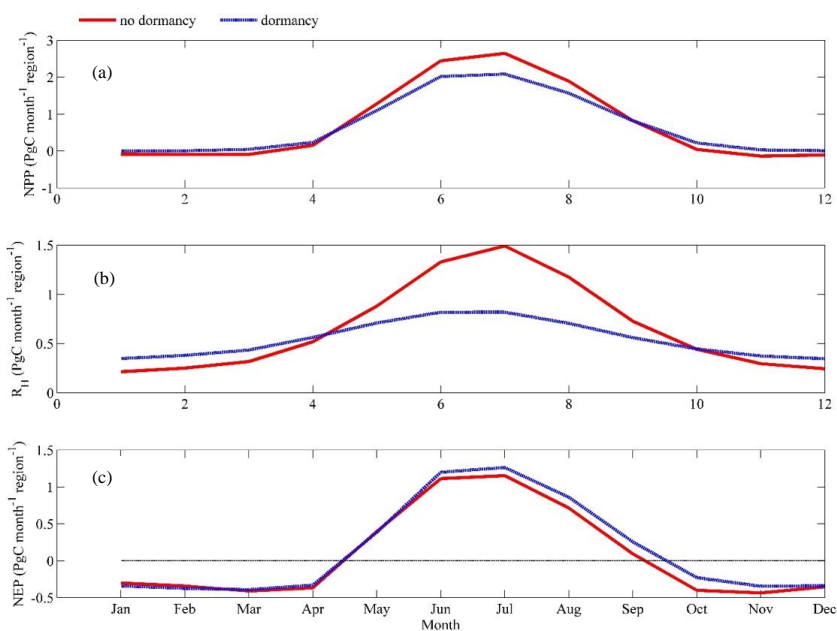


858
859 Figure 6. Linear regression between simulated and observed annual R_H (gC m⁻² yr⁻¹) for: (a) MIC-
860 TEM-dormancy, and (b) MIC-TEM.
861



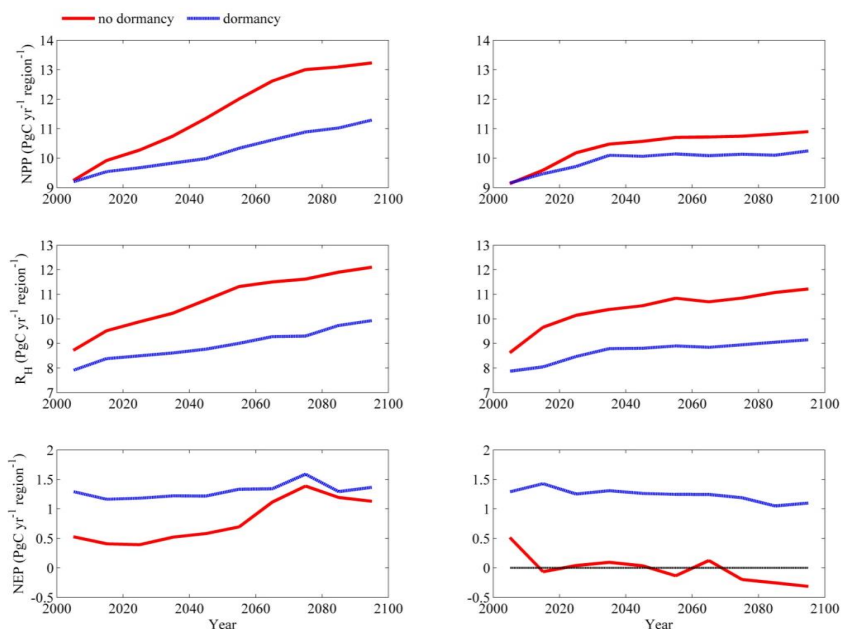
862

863 Figure 7. Simulated annual net primary production (NPP, top panel), heterotrophic respiration (R_H ,
864 center panel) and net ecosystem production (NEP, bottom panel) during the 20th century by
865 dormancy model and MIC-TEM, respectively.



866

867 Figure 8. Annual seasonal pattern of simulated (a) net primary production (NPP, top panel), (b)
868 heterotrophic respiration (R_H , center panel) and (c) net ecosystem production (NEP, bottom
869 panel) during the 1990s from dormancy model and MIC-TEM.



870

871 Figure 9. Predicted changes in carbon fluxes: (i) NPP, (ii) R_H , and (iii) NEP for all land areas north
872 of 45 °N in response to transient climate change under the RCP 8.5 scenario (left panel) and RCP
873 2.6 scenario (right panel) with dormancy model and MIC-TEM, respectively. The decadal running
874 mean is applied.

875
876

877

878

879

880

881

882

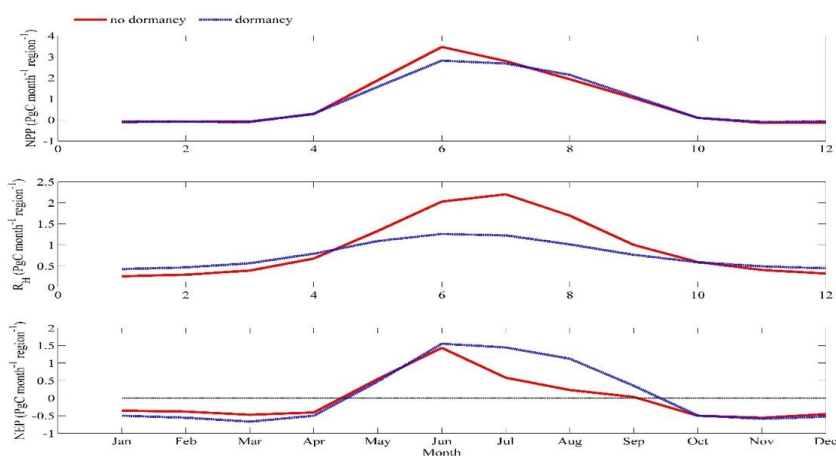
883

884

885

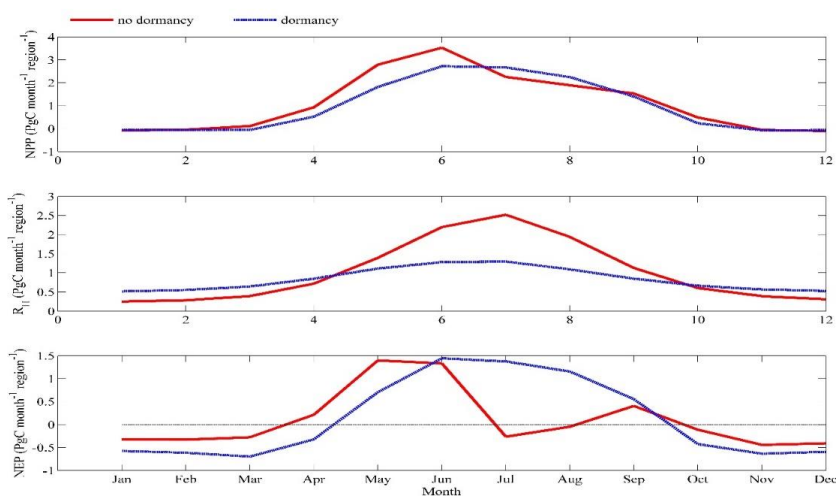


886 (a)



887

888 (b)



889

890 Figure 10. Annual seasonal pattern of simulated net primary production (NPP, top panel),
 891 heterotrophic respiration (R_H , center panel) and net ecosystem production (NEP, bottom panel)
 892 during the 2090s from dormancy model and MIC-TEM under: (a) RCP 2.6 scenario (top panel)
 893 and (b) RCP 8.5 scenario (bottom panel).

894

895



Table 1. Parameters associated with detailed microbial dormancy in MIC-TEM-dormancy

parameter	unit	description	Parameter range	references
m_R	h^{-1}	Specific maintenance rate at active state	[0.001, 0.08]	Wang et al. (2014)
Q_{10mic}	-	Temperature effects on microbial metabolic activity (rate change per 10 °C increase in temperature). Based on 0.65 eV activation energy for soils	[1.5, 3.5]	He et al. (2015)
Q_{10enz}	-	Temperature effects on enzyme activity (rate change per 10 °C increase in temperature). Based on 6% rate increase per degree Celsius	1.79	He et al. (2015)
α	-	the ratio of m_R to the sum of maximum specific growth rate	[0.01, 0.5]	Wang et al. (2014)
β	-	Ratio of dormant microbial maintenance rate to m_R	[0.0005, 0.005]	Wang et al. (2014)
Y_g	-	carbon use efficiency	[0.3, 0.7]	He et al. (2015)
K_s	$mgC\ cm^{-2}$	Half-saturation constant for directly accessible substrate	[0.01, 10]	Wang et al. (2014)
$K_{muptake}$	$mgC\ cm^{-2}$	Half-saturation constant for enzymatic decay of SOC	[200, 1000]	He et al. (2015)
r_{death}	h^{-1}	Potential rate of microbial death	[$2e^{-4}$, $2e^{-3}$]	Allison et al. (2010)
$r_{EnzProd}$	h^{-1}	Enzyme production rate of microbe	[$1e^{-4}$, $8e^{-4}$]	He et al. (2015)
$r_{enzloss}$	h^{-1}	Enzyme loss rate	[0.0005, 0.002]	Allison et al. (2010)
V_{max}	$mgC\ cm^{-2}\ h^{-1}$	Maximum SOC decay rate	[$1e^{-4}$, $5e^{-3}$]	He et al. (2015)

896
897

898
899
900



901 **Table 2. Site description and measured NEP data used to calibrate MIC-TEM-dormancy**

Site Name	Location (Longitude (degrees) /Latitude (degrees))	Elevation (m)	Vegetation type	Description	Data range	Citations
Univ. of Mich. Biological Station	84.71W 45.56 N	234	Temperate deciduous forest	Located within a protected forest owned by the University of Michigan. Mean annual temperature is 5.83°C with mean annual precipitation of 803mm	01/2005- 12/2006	Gough et al. (2013)
Howland Forest (main tower)	68.74W 45.20N	60	Temperate coniferous forest	Closed coniferous forest, minimal disturbance.	01/2004- 12/2004	Davidson et al. (2006)
UCL-1964 burn site	98.38W 55.91N	260	Boreal forest	Located in a continental boreal forest, dominated by black spruce trees, within the BOREAS northern study area in central Manitoba, Canada.	01/2004- 10/2005	Goulden et al. (2006)
KUOM Turfgrass Field	93.19W 45.0N	301	Grassland	A low-maintenance lawn consisting of cool-season turfgrasses.	01/2006- 12/2008	Hiller et al. (2011)
Atkasuk	157.41W 70.47N	15	Wet tundra	100 km south of Barrow, Alaska. Variety of moist-wet coastal sedge tundra, and moist-tussock tundra surfaces in the more well-drained upland.	01/2005- 12/2006	Oechel et al. (2014);
Ivotuk	155.75W 68.49N	568	Alpine tundra	300 km south of Barrow and is located at the foothill of the Brooks Range and is classified as tussock sedge, dwarf-shrub, moss tundra.	01/2004- 12/2004	McEwing et al. (2015)

902
 903
 904
 905



906 **Table 3. Site description and measured NEP data used to validate MIC-TEM-dormancy**

Site Name	Location (Longitude (degrees) /Latitude (degrees))	Elevation (m)	Vegetation type	Description	Data range	Citations
Bartlett Experimental Forest	71.29W/ 44.06N	272	Temperate deciduous forest	Located within the White Mountains National Forest in north-central New Hampshire, USA, with mean annual temperature of 5.61 °C and mean annual precipitation of 1246mm.	01/2005- 12/2006	Jenkins et al. (2007); Richardson et al. (2007);
Howland Forest (main tower)	68.74W/ 45.20N	60	Temperate coniferous forest	Closed coniferous forest, minimal disturbance.	01/2003- 12/2003	Davidson et al. (2006)
UCI-1964 burn site	98.38W/ 55.91N	260	Boreal forest	Located in a continental boreal forest, dominated by black spruce trees, within the BOREAS northern study area in central Manitoba, Canada.	01/2002- 12/2003	Goulden et al. (2006)
Brookings	96.84W/ 44.35N	510	Grassland	Located in a private pasture, belonging to the Northern Great Plains Rangelands, the grassland is representative of many in the north central United States, with seasonal winter conditions and a wet growing season.	01/2005- 12/2006	Gilmanov et al. (2005)
Atkasuk	157.41W/ 70.47N	15	Wet tundra	100 km south of Barrow, Alaska. Variety of moist-wet coastal sedge tundra, and moist-tussock tundra surfaces in the more well-drained upland.	01/2003- 12/2004	Oechel et al. (2014);
Ivotuk	155.75W/ 68.49N	568	Alpine tundra	300 km south of Barrow and is located at the foothill of the Brooks Range and is classified as tussock sedge, dwarf-shrub, moss tundra.	01/2005- 12/2005	McEwing et al. (2015)

908



Table 4. Site description and measured R_H data used to validate MIC-TEM-dormancy model

Site	Location (Longitude (degrees) /Latitude (degrees))	Elevation (m)	Vegetation type	Data range	Citations
US-EML	149.25W/ 63.88N	700	Alpine tundra	01/2009- 12/2013	Belshe et al. (2012)
CA-SJ2	104.65W/ 53.95N	580	Boreal forest	01/2004- 12/2008	Coursolle et al. (2006)
US-Ho2	68.75W/ 45.21N	91	Temperate coniferous forest	01/2000- 12/2004	Davidson et al. (2006)
US-UMB	84.71W/ 45.56N	234	Temperate deciduous forest	01/2005- 12/2006	Gough et al. (2013)
US-Ro4	93.07W/ 44.68N	274	Grasslands	01/2016- 12/2017	Griffis et al. (2011)
RU-Che	161.34E/ 68.61N	6	Wet tundra	01/2002- 12/2005	Merbold et al. (2009)

909
 910
 911
 912
 913
 914
 915
 916
 917
 918
 919
 920
 921



Table 5. Model validation statistics for Dormancy model and MIC-TEM at six sites with NEP data

Site Name	Vegetation type	Models	Intercept	Slope	R-square	Adjusted R-square	p-value
Ivotuk	Alpine tundra	MIC-TEM	0.85	0.83	0.70	0.67	<0.001
		Dormancy	-0.51	1.09	0.75	0.73	<0.001
UCI-1964 burn site	Boreal forest	MIC-TEM	0.18	1.03	0.912	0.9080	<0.001
		Dormancy	-0.21	0.96	0.90	0.894	<0.001
Howland Forest (main tower)	Temperate coniferous forest	MIC-TEM	7.29	0.72	0.85	0.83	<0.001
		Dormancy	0.27	1.05	0.89	0.88	<0.001
Bartlett Experimental Forest	Temperate deciduous forest	MIC-TEM	-6.05	0.91	0.944	0.941	<0.001
		Dormancy	-2.34	1.13	0.93	0.924	<0.001
Brookings	Grassland	MIC-TEM	3.05	0.71	0.84	0.83	<0.001
		Dormancy	0.17	0.95	0.90	0.898	<0.001
Atqasuk	Wet tundra	MIC-TEM	7.22	1.85	0.71	0.70	<0.001
		Dormancy	0.19	0.82	0.67	0.66	<0.001

922
 923
 924
 925
 926
 927
 928
 929
 930
 931
 932
 933
 934
 935
 936
 937
 938



Table 6. Model validation statistics for Dormancy model and MIC-TEM at six sites with R_H data

Site ID	Vegetation type	Models	Intercept	Slope	R-square	Adjusted R-square	RMSE	p-value
US-EML	Alpine tundra	MIC-TEM	2.90	0.91	0.79	0.78	3.55	<0.001
		Dormancy	1.81	0.74	0.87	0.85	2.69	<0.001
CA-SJ2	Boreal forest	MIC-TEM	7.59	1.12	0.84	0.83	9.8	<0.001
		Dormancy	2.6	0.74	0.86	0.85	3.97	<0.001
US-Ho2	Temperate coniferous forest	MIC-TEM	4.07	0.89	0.86	0.84	12.39	<0.001
		Dormancy	6.59	0.71	0.91	0.89	11.83	<0.001
US-UMB	Temperate deciduous forest	MIC-TEM	-4.73	1.32	0.81	0.8	20.05	<0.001
		Dormancy	13.6	0.67	0.85	0.84	12.94	<0.001
US-Ro4	Grassland	MIC-TEM	9.34	0.87	0.81	0.79	11.25	<0.001
		Dormancy	4.81	0.65	0.86	0.84	9.21	<0.001
RU-Che	Wet tundra	MIC-TEM	2.5	0.67	0.72	0.71	6.24	<0.001
		Dormancy	1.96	0.77	0.81	0.79	5.95	<0.001